Articles

Binding of Specialty Phosphines to Metals: Synthesis, Structure, and Solution Calorimetry of the Phosphirane Complex [PtMe₂(iPrBABAR-Phos)₂]

Cécile Laporte, Gilles Frison, and Hansjörg Grützmacher*

Chemistry Department HCI H131, ETH-Hönggerberg, CH-8093 Zürich, Switzerland

Anna C. Hillier, William Sommer, and Steven P. Nolan

Department of Chemistry, University of New Orleans, New Orleans, Louisiana 70148

Received August 8, 2002

The complex [PtMe₂(iPrBABAR-Phos)₂] (**3**) was prepared in a clean and quantitative ligand substitution reaction from [PtMe₂(cod)] (**1**; cod = η^4-1,5-cyclooctadiene) and the phosphirane iPrBABAR-Phos (**2**). The structure of **3** was determined by X-ray diffraction. The Pt−P bonds (~2.26 Å) lie in the shorter range of Pt^{II}−P bonds, although the $^1J(^{195}Pt^{31}P)$ coupling (1840 Hz) is quite small. The enthalpy for this ligand substitution reaction was measured by solution calorimetry and found to be exothermic by 11.8 kcal/mol, a relatively low exothermicity for a reaction involving a tertiary phosphine in this Pt system. Calculations using density functional theory (DFT) on the B3LYP level were applied using the simplified model reaction [PtH₂(cod)] + 2(H₂N)PC₂H₄ → [PtH₂{(H₂N)PC₂H₄}₂)] + cod, and these also gave a rather low substitution enthalpy (−17 kcal/mol). A charge decomposition analysis (CDA) was performed for Pt(II) and Pt(0) complexes with the simple *P*-amino phosphirane (H₂N)PC₂H₄ and PH₃ as ligands. Contrary to expectations, it is found that the phosphirane acts as a relatively good electron donor, while its electron-acceptor properties are not significantly different from those of other phosphines. The particularly low reaction enthalpy may thus be due to a low directionality of the donor orbitals toward the metal center.

Introduction

Phosphiranes contain a three-membered heterocycle with at least one phosphorus atom.[1−3] The sum of bond angles at the phosphorus center is small (<260°), which confers particular properties to these molecules; among these, their resistance to oxidation is the most noteworthy for practical reasons. In the past few decades a number of metal complexes were prepared with phosphiranes as ligands in various research groups.[1−6] We had developed the synthesis of BABAR-Phos, a phosphirane derivative in which the PC₂ cycle is incorporated into a polycyclic framework and which is easily prepared from simple starting materials.[7] Monocyclic phosphiranes tend to form metallaphosphetanes as the

more stable products with electron-rich metals via an insertion of the metal center into one P−C bond.[8−10] BABAR-Phos, on the other hand, allows the synthesis of fairly stable Rh(I) and Pt(0) complexes which are active hydrosilylation[11] and recyclable hydroboration catalysts.[12] Also, the metallaphosphetane formation with BABAR-Phos was found to be reversible and controllable by the coligands.

Given the utility of BABAR-Phos, we became interested in evaluating the binding energy as one key parameter for complex stability. A priori, it is not expected that phosphiranes would be strong σ-donors, because the donor orbital localized at the phosphorus

(1) Mathey, F.; Regitz, M. In *Phosphorus Heterocyclic Chemistry: The Rise of a New Domain*; Mathey, F., Ed.; Pergamon: Amsterdam, 2001; pp 17−55.
(2) Dillon, K. B.; Mathey, F.; Nixon, J. F. *Phosphorus: The Carbon Copy*; Wiley: New York, 1998; p 182.
(3) Mathey, F. *Chem. Rev.* **1990**, *90*, 997.
(4) Mézailles, N.; Fanwick, P. E.; Kubiak, C. P. *Organometallics* **1997**, *16*, 1526.
(5) Marinetti, A.; Mathey, F.; Ricard, L. *Organometallics* **1993**, *12*, 1207.
(6) Ajulu, F. A.; Hitchcock, P. B.; Mathey, F.; Michelin, R. A.; Nixon, J. F.; Pombeiro, A. J. L. *J. Chem. Soc., Chem. Commun.* **1993**, 142 and references cited therein.

(7) Liedtke, J.; Loss, S.; Alcaraz, G.; Gramlich, V.; Grützmacher, H. *Angew. Chem.* **1999**, *110*, 1724; *Angew. Chem. Int. Ed.* **1999**, *38*, 1623.
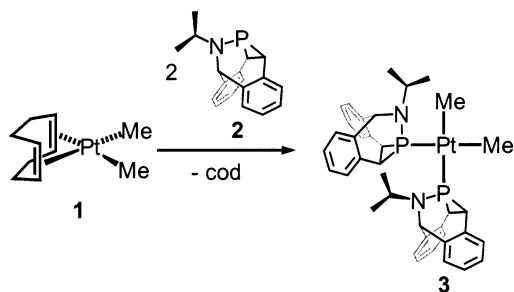(8) See: Carmichael, D.; Hitchcock, P. B.; Nixon, J. F.; Mathey, F.; Ricard, L. *J. Chem. Soc., Dalton Trans.* **1993**, 1811 and references cited therein.
(9) Ajulu, F. A.; Carmichael, D.; Hitchcock, P. B.; Mathey, F.; Meidine, M. F.; Nixon, J. F.; Ricard, L.; Riley, M. L. *J. Chem. Soc., Chem. Commun.* **1992**, 750.
(10) Al Juaid, S. S.; Carmichael, D.; Hitchcock, P. B.; Marinetti, A.; Mathey, F.; Nixon, J. F. *J. Chem. Soc., Dalton Trans.* **1991**, 905.
(11) Liedtke, J.; Loss, S.; Widauer, Ch.; Grützmacher, H. *Tetrahedron* **2000**, 56, 143 and references cited therein (Symposium in Print).
(12) Liedtke, J.; Rüegger, H.; Loss, S.; Grützmacher, H. *Angew. Chem.* **2000**, *112*, 2596; *Angew. Chem., Int. Ed.* **2000**, *39*, 2479.

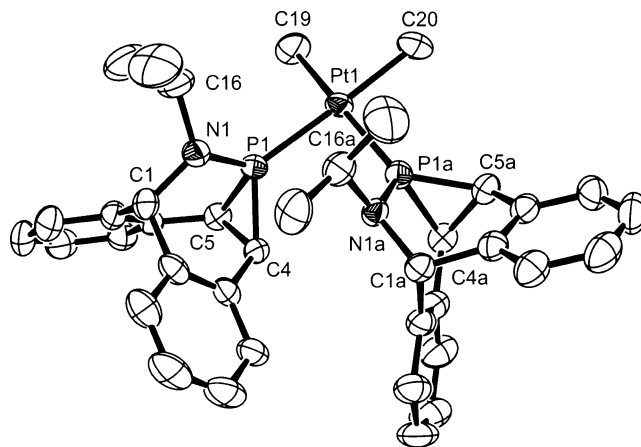**Scheme 1. Synthesis of [PtMe$_2$(^{iPr}BABAR-Phos)$_2$] (3)**

Figure 1. Molecular structure of **3**. Thermal ellipsoids are drawn at 50% probability; hydrogen atoms were omitted for clarity. Selected bond lengths (Å) and angles (deg) (the two phosphirane ligands show very similar structures, and averaged values are given here): Pt(1)−P(1) = 2.257(1), Pt(1)−P(1a) = 2.268(1), Pt(1)−C(19) = 2.090(4), Pt(1)−C(20) = 2.082(5), P(1/1a)−N(1/1a) = 1.676(4), P(1/1a)−C(4/4a) = 1.808(4), P(1/1a)−C(5/5a) = 1.828(4), C(4/4a)−C(5/5a) = 1.571(5), N(1/1a)−C(1/1a) = 1.485(5), N(1/1a)−C(16/16a) = 1.499(5); P(1)−Pt(1)−P(1a) = 90.36(4), C(20)−Pt(1)−C(19) = 86.3(2), C(19)−Pt(1)−P(1) = 91.51(15), C(20)−Pt(1)−P(1a) = 91.85(14), C(20)−Pt(1)−P(1) = 177.79-(14), C(19)−Pt(1)−P(1a) = 172.82(14), C(4/4a)−P(1/1a)−C(5/5a) = 51.2(2), N(1/1a)−P(1/1a)−C(4/4a) = 102.5(2), N(1/1a)−P(1/1a)−C(5/5a) = 103.7(2), N(1/1a)−P(1/1a)−Pt(1) = 123.0(1), C(4/4a)−Pt(1)−P(1/1a) = 123.1(2), C(5/5a)−P(1/1a)−Pt(1) = 130.6(1), C(5/5a)−C(4/4a)−P(1/1a) = 65.1(2), C(4/4a)−C(5/5a)−P(1/1a) = 63.8(2); Σ°(N) = 350.3, Σ°(P) = 257.4.

has high s-orbital character and hence is strongly contracted. On the other hand, phosphiranes may act as better π-acceptors as compared to other phosphines, because the strong pyramidalization of the P-coordination sphere leads to decreasing energies of unoccupied π-type orbitals which are mainly P−C antibonding in character.[10,13]

Results and Discussion

Synthesis and Structure of [PtMe$_2$(^{iPr}BABAR-Phos)$_2$]. As the system of choice, we investigated the reaction of [PtMe$_2$(cod)] (**1**) with ^{iPr}BABAR-Phos (**2**). The binding energy of various monodentate phosphines, PR$_3$,[14] and bis(chelates), R$_2$P−X−PR$_2$,[15] with **1** has been determined previously by solution calorimetry and therefore allows a ranking of the binding qualities of BABAR-Phos. Furthermore, these studies showed that the PtMe$_2$ fragment has neither predominant electron acceptor nor electron donor properties, which may be a useful quality for the evaluation of σ/π donor/acceptor properties of additional ligands. The reaction of **1** with 2 equiv of **2** in methylene chloride at room temperature proceeds smoothly and gives the Pt(II) ^{iPr}BABAR-Phos complex as the only product (Scheme 1).

After recrystallization, **3** is obtained as a white microcrystalline powder in about 87% isolated yield. In the ^{31}P NMR spectrum, one sharp resonance at −69.6 ppm is detected, accompanied by characteristic satellites separated by 1840 Hz due to coupling with the ^{195}Pt nucleus. The ^{31}P chemical shift is not significantly different from the ones observed in Pt(0) complexes with BABAR-Phos ligands[7,11] and is shifted by about 80 ppm to higher frequencies in comparison to the free ligand **2** (−153.5 ppm). While in the Pt(0)−BABAR-Phos complexes ^1J(^{195}Pt^{31}P) is rather large (>4200 Hz) and is in the upper range of known values, the ^{195}Pt^{31}P coupling in **3** is quite small and falls into the range which is typically observed for Pt(II) complexes with σ-donating alkyl-substituted phosphines. Pt(II) complexes with electron-poor/π-accepting phosphines frequently show larger couplings (>2000 Hz).[14,16] On the other hand, the platinum-bonded methyl groups are shifted to rather high frequencies (^{1}H NMR: 0.98 ppm, ^2J(^{195}Pt^{1}H) = 78.2 Hz) which is typical for Pt(II)

complexes with electron-poor phosphines such as pyr-rolylphosphines, P(pyrl)$_3$.[14]

Crystals suitable for X-ray analysis were grown from a concentrated CH$_2$Cl$_2$ solution layered with *n*-hexane. The result of the data refinement (see Table 3 in the Experimental Section) is shown in Figure 1. Because the individual bond lengths in the two coordinated BABAR-Phos ligands in **3** do not vary much, selected averaged bond lengths and angles are given in the caption to Figure 1. In the structure of **3**, the two methyl groups and the two BABAR-Phos ligands occupy cis positions in the expected square-planar coordination sphere of the d^8 valence electron configured Pt(II) center. For steric reasons, the isopropyl groups at the BABAR-Phos nitrogen center lie on the same side with respect to the central molecular plane, which we also observed for the cationic [Rh(^{iPr}BABAR-Phos)$_4$]$^+$ complex.[12] The lengths of the Pt−P bonds in **3** (2.257(1), 2.268(1) Å) are slightly shorter than those in Pt(II) alkylphosphine complexes and approach values observed in complexes with electron-poorer phosphines.

The platinum−methyl distances in **3** (2.082(5), 2.090(4) Å) are also in the lower range of previously observed lengths. Note, however, that the variations of the Pt−P and Pt−Me distances in [PtMe$_2$(PR$_3$)$_2$] and [PtMe$_2$(PP)] complexes (PP = chelating diphosphine) are in general comparatively small (Pt−P = 2.24−2.34 Å; Pt−Me = 2.07−2.26 Å) even for sterically and/or electronically rather different phosphines. To this end, we conclude therefore that no particular steric or electronic
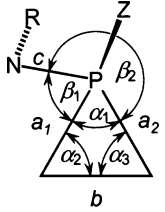
(13) Nguyen, M. T.; Van Praet, E.; Vanquickenborne, L. G. *Inorg. Chem.* **1994**, *33*, 1153.

(14) Haar, C. M.; Nolan, S. P.; Marshall, W. J.; Moloy, K. G.; Prock, A.; Giering, W. P. *Organometallics* **1999**, *18*, 474−479.

(15) Smith, D. C., Jr.; Haar, C. M.; Stevens, E. D.; Nolan, S. P. *Organometallics* **2000**, *19*, 1427−1433.

(16) Pregosin, P. S. *Annu. Rep. NMR Spectrosc.* **1986**, *17*, 285.

Table 1. Comparison of Pertinent Structural Parameters of (i) [BTMP]BABAR-Phos,[11a] (ii) [Pt(iPrBABAR-Phos)$_2$(PPh$_3$)$_2$],[7] (iii) [Pt(iPrBABAR-Phos)(dvtms)],[7,11] (iv) 3, and (v) a tBu−Phosphiranium Cation[11] (CN = Coordination Number)

Bond Lengths (Å)

Z^a	a_1	a_2	b	c
	1.850(3)	1.863(3)	1.532(4)	1.738(2)
Pt(0), CN 4	1.831(5)	1.856(5)	1.558(7)	1.699(4)
Pt(0), CN 3	1.812(6)	1.821(7)	1.576(9)	1.684(6)
Pt(II) **3**	1.808(4)	1.828(4)	1.571(5)	1.676(4)
tBu$^+$	1.774(3)	1.774(3)	1.601(6)	1.628(4)

Bond Angles (deg)

Z^a	α_1	α_2	α_3	β_1	β_2
	48.8(1)	66.0(2)	65.2(2)	98.8(1)	99.0(1)
Pt(0), CN 4	49.9(2)	64.2(2)	65.8(2)	99.5(2)	101.0(2)
Pt(0), CN 3	51.4(3)	64.0(3)	64.6(3)	101.7(3)	103.1(3)
Pt(II)	51.2(2)	65.1(2)	63.8(2)	102.5(2)	103.7(2)
tBu$^+$	53.6(2)	63.2(1)	63.2(1)	108.2(2)	108.2(2)

^{a} R = 3,5-bis(trifluoromethyl)phenyl (BTMP).

interactions are reflected in the metric parameters of the platinum coordination sphere.

For comparison, the structural parameters of the PC$_2$ cycle in (i) a noncomplexed BABAR-Phos (with 2,5-(CF$_3$)C$_6$H$_2$ instead of iPr at the nitrogen atom), (ii) in the four-coordinate Pt(0) complex [Pt(iPrBABAR-Phos)$_2$-(PPh$_3$)$_2$],[7] (iii) in the three-coordinate Pt(0) complex [Pt-(iPrBABAR-Phos)(dvtms)] (dvtms = divinyltetramethylsiloxane),[7,11] (iv) **3**, and (v) the *tert*-butylphosphiranium cation[11] are listed in Table 1.

As is generally observed for phosphines, the bonds from the phosphorus atom to its neighboring atoms, here the P−C bonds a_1 and a_2 and the P−N bond c, become shorter when the P lone pair is involved in bonding. Also, the bond angles α_1, β_1, and β_2 are widened. These effects are provoked by increasing electron donation from the phosphorus atom to its bonding partner Z, whereby the positive atomic charge at the P center increases. As the data in Table 1 show, the P→Z donation increases in the order Z = Pt(0) CN 4 < Pt(0) CN 3 < Pt(II) < tBu$^+$ (CN = coordination number), placing the complexes between the noncoordinated ligand and the phosphiranium salt in which the P→tBu$^+$ interaction can be regarded as pure donation. The structural data show that P→Pt electron donation makes a strong contribution to the electronic interaction of BABAR-Phos with platinum centers. If Pt→P back-donation plays a dominant role, P−C and P−N bond lengthening is expected (because the transfer of electron density from the metal to the phosphine PX$_3$ occurs in P−X antibonding orbitals).

Solution Calorimetry. The substitution reaction shown in Scheme 1 is clean and quantitative at $T = 298$ K at reaction times below 1 h. As is detailed in the Experimental Section, an enthalpy ΔH_r of -11.8 ± 0.2 kcal/mol was determined from several experiments,

Chart 1. Depiction of Structures Calculated at the B3LYP Density Functional Level of Theory^a
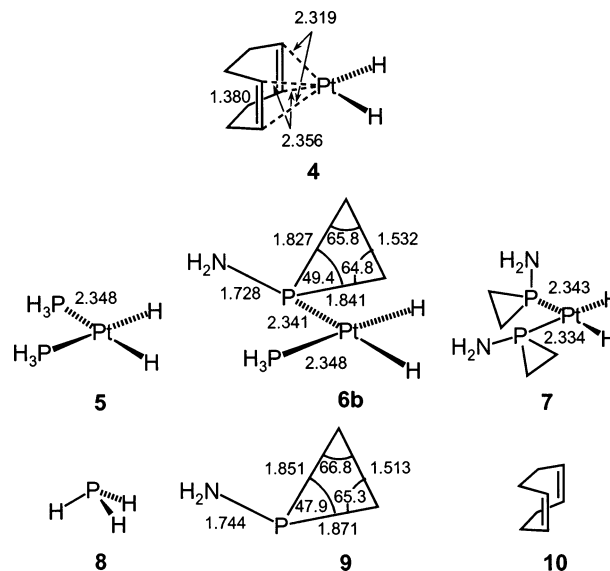
^{a} Selected bond lengths (Å) and angles are given for **4**, **5**, **6b**, and **9**.

which can be compared with substitution enthalpies for a series of structurally related [PtMe$_2$(PR$_3$)$_2$][14] and [PtMe$_2$(PP)][15] complexes that were obtained in a similar manner. In the series with the monodentate phosphines, the highest enthalpy, -34.3 ± 0.2 kcal/mol, was observed for PMe$_3$ as the sterically less demanding electron-donor phosphine and the lowest value, -19.2 ± 0.2 kcal/mol, was obtained for PCy$_3$ (Cy = cyclohexyl). This small binding energy is certainly caused by the high steric bulk. Note that electron-poor/π-accepting phosphines with "normal" steric requirements such as P(pyrl)$_3$ (pyrl = pyrrolyl) are also relatively weakly bound; i.e., $\Delta H_r = -20.4 \pm 0.2$ kcal/mol. As expected, for chelating bisphosphines in the series [PtMe$_2$(PP)], slightly higher binding enthalpies are found than with two monodentate phosphines. Also, alkyl-substituted derivatives give larger values ($> |-35|$ kcal/mol) than aryl-substituted ones and with (pyrl)$_2$P−(CH$_2$)$_2$−P(pyr)$_2$ the lowest value (-21.7 kcal/mol) was measured. To this end, BABAR-Phos gives by far the lowest substitution enthalpy measured to date.

Quantum-Chemical Calculations. Calculations were performed using B3LYP density functional theory (DFT) in order to gain additional insight into the electronic structure of platinum phosphirane complexes. In particular, we were interested in evaluating the binding quality of a phosphirane toward a Pt(II) center using charge decomposition analysis (CDA) as introduced by Frenking et al.[17] As detailed in the Experimental Section, this method corresponds to a "quantified" Dewar−Chatt−Duncanson model and gives information about the amount of L→M donation, d, L←M back-donation, b, and L↔M repulsive interactions, r. Second, we wanted to compute the substitution enthalpy for a model reaction close to the one we have investigated in Scheme 1. The model compounds we used for this investigation are depicted in Chart 1. As frequently observed, the distances from the metal to its neighboring

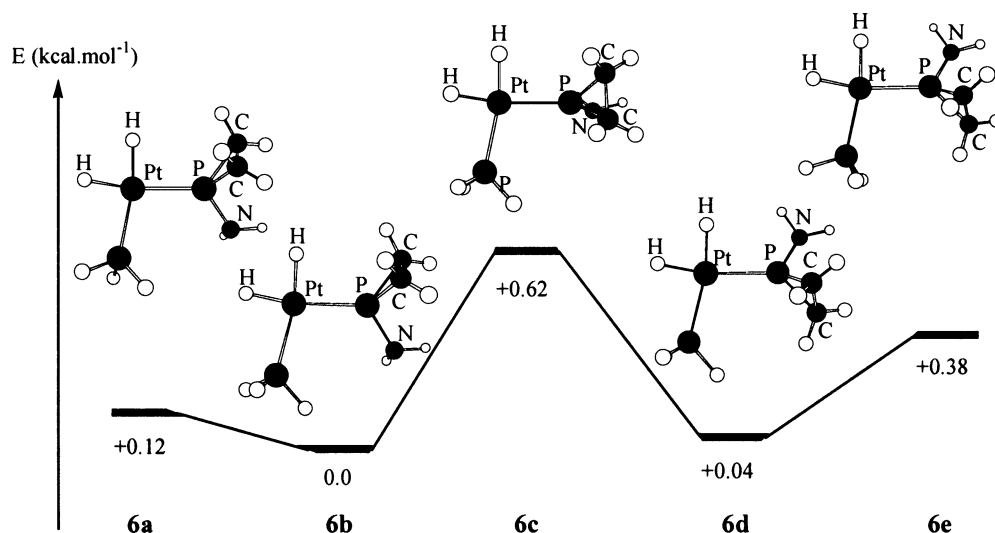(17) Dapprich, S.; Frenking, G. *J. Phys. Chem.* **1995**, *99*, 9352.

Figure 2. Comparison of PH_3 and $(H_2N)PC_2H_4$ rotation barriers relating the conformers **6b** and **6d** at the B3LYP level of theory.

Table 2. Charge Decomposition Analysis[a] and Interaction Energy E_{int} (in kcal/mol) for the Phosphines PH_3 (8) and $(H_2N)PC_2H_4$ (9) in Platinum(II) (entries 1 and 2) and Platinum(0) Complexes (entries 3 and 4) Calculated at the B3LYP/II Level

entry no.	phosphane/complex	d	b	d/b	r	Δ	E_{int}
1	PH_3 (**8**)/**6b**	0.461	0.171	2.70	−0.379	0.004	32.0
2	$(H_2N)PC_2H_4$ (**9**)/**6b**	0.598	0.203	2.95	−0.274	−0.018	34.1
3	PH_3 (**8**)/**6c**	0.454	0.180	2.52	−0.383	0.004	32.3
4	$(H_2N)PC_2H_4$ (**9**)/**6c**	0.604	0.219	2.76	−0.272	−0.019	34.4
5	PH_3 (**8**)/[$Pt(PH_3)_3$] (**11**)[19]	0.382	0.229	1.67	−0.597	0.020	28.3
6	$(H_2N)PC_2H_4$ (**9**)/[$Pt(PH_3)_2\{(H_2N)PC_2H_4\}$] (**12**)	0.494	0.275	1.80	−0.342	−0.038	31.1

[a] Donation d, back-donation b, repulsive polarization r, and residual term Δ.

atoms are all slightly too long in the B3LYP calculations in comparison with X-ray crystallographic structures.[18] Gross structural features are, however, correctly represented, as the $Pt-P_{phosphirane}$ bonds in **6b** or **7** are found to be slightly shorter than the $Pt-PH_3$ bonds in **5** or **6b** and the overall agreement of the calculated structures with experiment is satisfying. In particular, the structural changes within the phosphirane unit upon complexation are reproduced: i.e., the P−C and P−N bonds becoming shorter and the C−C bond of the PC_2 cycle becoming longer when **9** is coordinated. Also, the C−P−C angle is widened, while the inner-ring P−C−C angles are narrowed when the phosphirane **9** is coordinated.

For the CDA, the mixed [$PtH_2(PH_3)(H_2NPC_2H_4)$] complex **6** seemed especially interesting because an internal comparison of the model phosphirane (H_2N)-PC_2H_4 (**9**) versus the phosphine PH_3 (**8**) is possible. Both phosphines are exposed to the strong trans influence of a hydride ligand, while their mutual influence should be small, being bonded in cis positions. Searching on the potential energy surface (PES) for the most stable structure of **6**, we found two stable rotational conformers, denoted as **6b** and **6d** in Figure 2, which differ by only 0.04 kcal/mol. In both conformers, the PC_2 cycle adopts a position such that the nitrogen atom of the NH_2 group lies almost in the central molecular plane including the phosphorus atoms, hydrogen atoms, and the

platinum atom. This observation was made also for Pt(0) complexes with monosubstituted phosphines PH_2R with R ≠ H.[19] However, the barrier for rotation around the Pt−P(phosphirane) bond via the transition state (TS) **6c** is very low (0.62 kcal/mol) and is not significantly higher than the rotation barrier for the PH_3 ligand in **6b** (via TS **6a** at 0.12 kcal/mol) or **6d** (via TS **6e** at 0.38 kcal/mol). This finding can be interpreted in terms of the absence of any particular π-interaction between the phosphirane **9** and the $(PH_3)PtH_2$ fragment (neither π-donation or π-acception) in one specific plane of the complex.

We discuss here the results of the CDA for the most stable complex, **6b**, although the structure **6c** is closer to the experimental structure in the sense that the nitrogen atom does not lie in the central plane of the complex. However, the CDA gives very similar results, as indicated in Table 2. The calculated values for donation, d, back-donation, b, and repulsion, r, for the PH_3 ligand **8** (entries 1 and 3) and phosphirane ligand **9** are listed in Table 2. In all cases, the residual term Δ is small, which is a prerequisite to allow a meaningful discussion. For comparison we have also included the data for the tris(phosphine) Pt(0) complex [$Pt(PH_3)_3$] (**11**)[19] and the bis(phosphine) phosphirane complex [$Pt(PH_3)_2\{(H_2N)PC_2H_4\}$] (**12**).

In contrast to our expectations, we find that L→M donation, d, increases more than L←M back-donation, b, on going from PH_3 (**8**) to $(H_2N)PC_2H_4$ (**9**). As a net effect the d/b ratio for **9** is larger than for **8**, and this is

(18) For Pt(0) phosphine complexes the Pt−P bonds are about 0.03−0.05 Å longer than the lengths determined experimentally; see: Udin, J.; Dapprich, S.; Frenking, G.; Yates, B. F. *Organometallics* **1999**, *18*, 458.

(19) Frison, G.; Grützmacher, H. *J. Organomet. Chem.* **2002**, *643−644*, 285.

Chart 2. Substitution Reactions Transforming [PtH$_2$(cod)] (4) Successively into [PtH$_2$(PH$_3$)$_2$] (5) → [PtH$_2$(PH$_3$){(H$_2$N)PC$_2$H$_4$}] (6b) → [PtH$_2${(H$_2$N)PC$_2$H$_4$}$_2$] (7)^a
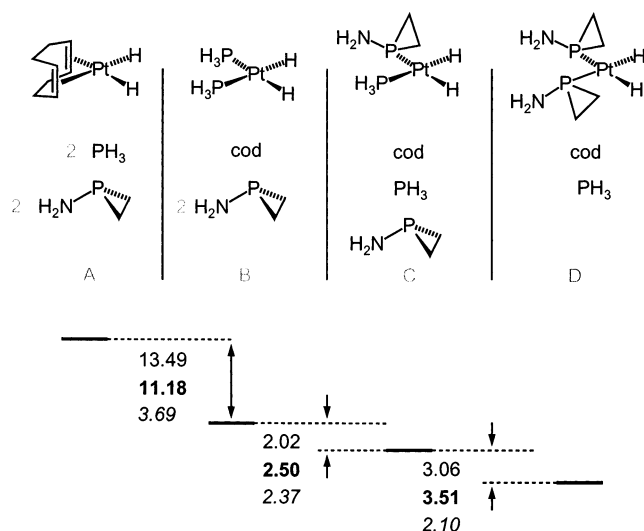
^{a} Relative energies, enthalpies (in boldface), and free energies (in italics) are given in kcal/mol. Enthalpies and free energies are given at $T = 298$ K.

true for Pt(II) and Pt(0). Given that PH$_3$ is an especially bad acceptor, d/b will be even smaller for other phosphines, making the difference between them and **9** even larger.[19,20] We find that the d/b ratio is smaller for Pt(0); i.e., back-donation becomes relatively more important with the lower oxidized metal center in accord with qualitative bonding models. Note that also the intrinsic reaction energy, E_{int}, is higher for the phosphirane **9** than for PH$_3$, regardless of the platinum oxidation state. (E_{int} corresponds to the interaction energy of the metal fragment ML$_n$ with the ligand L when both have already adopted the structure within the complex; i.e., they are electronically and structurally prepared for bonding.)

To get a better picture of the thermodynamic substitution energies, we calculated the reactions outlined in Chart 2. The first step in our model reaction sequence is the substitution of the cyclooctadiene (cod) ligand in [PtH$_2$(cod)] (**4**) by two PH$_3$ ligands, which is modestly exothermic ($\Delta H_r = -11.18$ kcal/mol). The stepwise substitution of each PH$_3$ (**8**) by (H$_2$N)PC$_2$H$_4$ (**9**) is slightly exothermic for each step by -2.50 and -3.51 kcal/mol, respectively, leading to an overall reaction enthalpy of about -17 kcal/mol, which is in reasonable accord with the experimentally derived value.

The calculations show that phosphirane **9** is a stronger ligand than PH$_3$, which, however, is an especially poorly bonded phosphine. Any other phosphine will be a significantly stronger ligand. Also, the binding energy will increase in the series PH$_2$R < PHR$_2$ < PR$_3$ and therefore especially tertiary phosphines will be more strongly bound to the PtH$_2$ fragment than a phosphirane.[20]

In accordance with the results from the solution calorimetry and the DFT calculations are the following simple substitution reactions, which we performed in an NMR tube. Addition of 2 equiv of P(OMe)$_3$, P(OPh)$_3$,

or PPh$_3$ to a CH$_2$Cl$_2$ solution of [PtMe$_2$(^{iPr}BABAR-Phos)$_2$] (**3**) rapidly (<10 min) and quantitatively leads to a displacement of the two BABAR-Phos ligands and formation of [PtMe$_2$(PR$_3$)$_2$] (R = OMe,[21] δ(^{31}P) 137.9, $^1J_{PtP} = 3120$ Hz; R = OPh, δ(^{31}P) 119.7, $^1J_{PtP} = 3058$ Hz; R = Ph,[22] δ(^{31}P) 26.7, $^1J_{PtP} = 1899$ Hz). The intermediate formation of the mixed complex [PtMe$_2$(BABAR-Phos){PPh$_3$}] (δ(^{31}P) -61.1, $^1J_{PtP} = 2002$ Hz, $^2J_{PP} = 13$ Hz (BABAR-Phos); δ(^{31}P) 23.1, $^1J_{PtP} = 1843$ Hz, $^2J_{PP} = 13$ Hz (PPh$_3$)) was only observed with PPh$_3$, where the reaction is slightly slower.

Conclusion. The thermochemical determination of the substitution enthalpy, ΔH_r, for the reaction between [PtMe$_2$(cod)] (**1**) and ^{iPr}BABAR-Phos (**2**), yielding [PtMe$_2$(^{iPr}BABAR-Phos)$_2$] (**3**), resulted in the lowest value (-11.8 kcal/mol) ever observed for a phosphine. Accordingly, the BABAR-Phos ligands in **3** are readily displaced by other phosphines. Since the Pt–P bonds in **3** are rather short and lie in the lower region of Pt–P bonds, the above reaction gives another example for the "short bond–low substitution enthalpy" paradox. This does not necessarily mean that the M–P bonds are intrinsically weak, since thermochemical measurements give only the difference between states.[14,15,23] However, since no strong particular steric interactions are recognized in the ligand sphere of complex **3** and the structural changes in the free and complexed form of the ligand are small,[24] the low enthalpy is most likely connected with a low Pt–P binding energy. A CDA analysis shows that phosphiranes are not especially poor electron donors or significantly strong electron acceptors. This is indicated by the absence of a sizable rotation barrier for the phosphirane (H$_2$N)PC$_2$H$_4$ (**9**) in the complex [Pt(PH$_3$){(H$_2$N)PC$_2$H$_4$}] (**6b**). Although more substantiated conclusions must await a more detailed theoretical analysis using a larger set of various types of phosphines, we ascribe the particularly low binding enthalpy for phosphiranes such as BABAR-Phos to the fact that the donor orbitals (mainly the s and p orbitals at phosphorus corresponding approximately to the lone pair and the P–C bonds of the PC$_2$ ring plane perpendicular to the P–M axis) are only poorly directed toward the metal center. This results in a poor overlap and low binding energy, although the M–P bonds may be rather short. However, further investigations are needed to allow a generalization of the observations reported here.

(20) Frison, G.; Grützmacher, H.; Frenking, G. Unpublished results.

(21) Yang, D.-S.; Bancroft, G. M.; Dignard-Bailey, L.; Puddephatt, R. J.; Tse, J. S. *Inorg. Chem.* **1990**, *29*, 2487–2495.

(22) Rashidi, M.; Fakhroeian, Z.; Puddephatt, R. J. *J. Organomet. Chem.* **1991**, *406*, 261–268.

(23) Huang, J.; Haar, C. M.; Nolan, S. P.; Marshall, W. J.; Moloy, K. G. *J. Am. Chem. Soc.* **1998**, *120*, 7806–7815 and references cited therein.

(24) For the ensemble of reactions [PtMe$_2$(cod)] + 2PR$_3$ → [PtMe$_2$(PR$_3$)$_2$] + cod, the contributions to the reaction enthalpy which are caused by structural differences of the PtMe$_2$ fragments on the left and right sides of the reaction equation and the free and bonded forms of cod should be almost equal. The contributions which are evoked by different conformations of the substituents R in the free and complexed forms of the phosphines are difficult to evaluate. However, as we discussed above, we have no indication of any unfavorable steric interactions of the BABAR-Phos ligands in the coordination sphere of **3**. Furthermore, BABAR-Phos molecules have a very rigid structure, which does not change much upon complexation. This can be shown by the comparison between a number of related BABAR-Phos ligands and their complexes, whose structures we determined by X-ray analyses (Liedtke, J. ETH-Dissertation No. 13688, 2000). Therefore, it can be assumed that the small enthalpy reported here is mainly due to a low Pt–P binding energy.

Experimental Section

Theoretical Methods. Full geometry optimizations for systems **4**−**10** were carried out with the use of the B3LYP[25,26] density functional level of theory and with the following basis set. The Hay and Wadt small-core relativistic effective-core potential with a valence shell of double-ζ quality (441/2111/21) was used on platinum.[27] The 6-31G(d) basis set[28,29] was employed for all the other atoms, except for the hydrogen atoms located on the platinum center, for which a set of 2p polarization functions (6-31G(d,p) basis set) were added. Sets of six Cartesian d functions were used in the basis sets throughout these calculations. This corresponds to the standard "Basis Set II" defined by Frenking and collaborators,[30] and the level of theory used in this study will hereafter thus be denoted as B3LYP/II. The optimized structures were characterized by harmonic frequency analysis as minima (all frequencies real; **4**, **5**, **6b,d**, **7**−**10**) or transition states (only one imaginary frequency; **6a,c,e**). These molecular orbital calculations were performed with the Gaussian 98 programs.[31]

Total energies have been computed at the level of optimization (B3LYP/II). The zero-point, thermal, and entropic corrections from the B3LYP analyses were used, without scaling to convert, in some cases, the B3LYP electronic energies to enthalpies and free energies at 298 K.[32]

Metal−ligand donor−acceptor interactions were examined in terms of charge donation, back-donation, and repulsive polarization using the program CDA 2.1.[33] This charge decomposition analysis (CDA)[17] is achieved by inspecting the orbital contributions to the charge distributions in the complex by (i) the mixing of the filled orbitals of the ligand, L, with the unfilled orbitals at the metal-containing fragment, $[ML^1{}_n]$ (donation, d), (ii) the mixing of the unfilled orbitals of L with the filled orbitals at $[ML^1{}_n]$ (back-donation, b), (iii) the mixing of the filled orbitals of L with the filled orbitals at $[ML^1{}_n]$ (repulsive polarization, r), and (iv) the mixing of the unfilled orbitals of L with the unfilled orbitals at $[ML^1{}_n]$ (residual term, Δ).

Total energies and complete sets of Cartesian coordinates for the optimized geometries are contained in the Supporting Information.

Experimental Methods. (a) General Considerations. All manipulations involving organoplatinum complexes were performed under an inert atmosphere of argon, using standard

Table 3. Crystal Data and Structure Refinement Details for the Complex [Pt^{II}(^{i}Pr$BABAR$-Phos)$_2$(CH$_3$)$_2$] (3)

identification code	0_75
empirical formula	$C_{38}H_{42}N_2P_2Pt$
temp	293(2) K
wavelength	0.710 73 Å
cryst syst	monoclinic
space group	$P2_1/n$
unit cell dimens	
a	13.0620(10)
b	12.5170(10)
c	20.4639(14)
α	90
β	92.990(3)
γ	90
V	3341.2(4) Å^3
Z	4
calcd density	1.558 Mg/m^3
abs coeff	4.324 mm^{-1}
F(000)	1568
cryst size	$0.5 \times 0.5 \times 0.2$ mm
data collection	Siemens SMART PLATFORM with CCD detector, graphite monochromator
detector dist	30 mm
method; exposure time/frame	ω scans; $t = 10$ s
refinement method	full-matrix least squares on F^2, SHELXL97
θ range for data collection	1.81−28.28°
index ranges	$-17 \leq h \leq 13$, $-16 \leq k \leq 16$, $-22 \leq l \leq 27$
no. of rflns collected	28 328
no. of indep rflns	8286 (R(int) = 0.0726)
abs cor	empirical (SADABS)
no. of data/restraints/params	8286/0/388
goodness of fit on F^2	0.999
final R indices ($I > 2\sigma(I)$)	R1 = 0.0360, wR2 = 0.0687
R indices (all data)	R1 = 0.0594, wR2 = 0.0715
largest diff peak and hole	2.169 and -1.823 e Å^{-3}

high-vacuum or Schlenk techniques, or in a MBraun glovebox containing less than 1 ppm of oxygen and water. Only materials of high purity as indicated by NMR spectroscopy were used in the calorimetric experiments. The NMR spectra were recorded on a Bruker DPX 250 MHz or DPX 300 MHz spectrometer. ^{1}H and ^{13}C chemical shifts are calibrated against the solvent signal (CDCl$_3$, ^{1}H NMR 7.27 ppm, ^{13}C NMR 77.23 ppm; CD$_2$Cl$_2$, ^{1}H NMR 5.32 ppm, ^{13}C NMR 54.00 ppm). ^{31}P chemical shifts are calibrated against 85% H$_3$PO$_4$ as an external standard. Calorimetric measurements were performed using a Calvet calorimeter (Setaram C-80), which was periodically calibrated using the Tris reaction[34] or the enthalpy of solution of KCl in water.[35] The calorimeter has been previously described.[36,37] The experimental enthalpies for these two standard reactions compared very closely to literature values. The phosphine ligand used in this study was prepared by the literature method.[7]

(b) NMR Titrations. Prior to every set of calorimetric experiments involving a ligand, a precisely measured amount (± 0.1 mg) of [PtMe$_2$(cod)] (**1**) was placed in an NMR tube along with CD$_2$Cl$_2$ and 2.1 equiv of ligand. Both ^{1}H and ^{31}P{^{1}H} NMR spectra were measured within 1 h of mixing; both indicated the reactions were clean and quantitative. These conditions are necessary for accurate and meaningful calorimetric results and were satisfied for all reactions investigated.

(c) Solution Calorimetry. In a representative experiment, the mixing vessels of the Setaram C-80 instrument were

(25) Lee, C.; Yang, W.; Parr, R. G. *Phys. Rev.* **1988**, *B37*, 785.

(26) Becke, A. D. *J. Chem. Phys.* **1993**, *98*, 5648.

(27) Hay, P. J.; Wadt, W. R. *J. Chem. Phys.* **1985**, *82*, 299.

(28) Hariharan, P. C.; Pople, J. A. *Theor. Chim. Acta* **1973**, *28*, 213.

(29) Francl, M. M.; Petro, W. J.; Hehre, W. J.; Binkley, J. S.; Gordon, M. S.; DeFrees, D. J.; Pople, J. A. *J. Chem. Phys.* **1982**, *77*, 3654.

(30) Frenking, G.; Antes, I.; Böhme, M.; Dapprich, S.; Ehlers, A. W.; Jonas, V.; Neuhaus, A.; Otto, M.; Stegmann, R.; Veldkamp, A.; Vyboishchikov, S. F. In *Reviews in Computational Chemistry*; Lipkowitz, K. B., Boyd, D. B., Eds.; VCH: New York, 1996; Vol. 8, pp 63−144.

(31) Frisch, M. J.; Trucks, G. W.; Schlegel, H. B.; Scuseria, G. E.; Robb, M. A.; Cheeseman, J. R.; Zakrzewski, V. G.; Montgomery, J. A., Jr.; Stratmann, R. E.; Burant, J. C.; Dapprich, S.; Millam, J. M.; Daniels, A. D.; Kudin, K. N.; Strain, M. C.; Farkas, O.; Tomasi, J.; Barone, V.; Cossi, M.; Cammi, R.; Mennucci, B.; Pomelli, C.; Adamo, C.; Clifford, S.; Ochterski, J.; Petersson, G. A.; Ayala, P. Y.; Cui, Q.; Morokuma, K.; Malick, D. K.; Rabuck, A. D.; Raghavachari, K.; Foresman, J. B.; Cioslowski, J.; Ortiz, J. V.; Stefanov, B. B.; Liu, G.; Liashenko, A.; Piskorz, P.; Komaromi, I.; Gomperts, R.; Martin, R. L.; Fox, D. J.; Keith, T.; Al-Laham, M. A.; Peng, C. Y.; Nanayakkara, A.; Gonzalez, C.; Challacombe, M.; Gill, P. M. W.; Johnson, B. G.; Chen, W.; Wong, M. W.; Andres, J. L.; Head-Gordon, M.; Replogle, E. S.; Pople, J. A. *Gaussian 98*, revision A.9; Gaussian, Inc.: Pittsburgh, PA, 1998.

(32) It has to be remembered that the accuracy of computed entropic contributions to the free energies are suspect, due to the fact that (a) gas-phase entropies are not the same as the solution-phase entropies, which are chemically relevant, and (b) Gaussian 98 uses harmonic oscillator partition functions for the low-frequency, hindered rotations in the complexes.

(33) Dapprich, S.; Frenking, G. CDA 2.1; Marburg, Germany, 1994.

(34) Ojelund, G.; Wadsö, I. *Acta Chem. Scand.* **1968**, *22*, 1691−1699.

(35) Kilday, M. V. *J. Res. Natl. Bur. Stand. (U.S.)* **1980**, 85, 467−481.

(36) Nolan, S. P.; Hoff, C. D.; Landrum, J. T. *J. Organomet. Chem.* **1985**, *282*, 357−362.

(37) Nolan, S. P.; Lopez de la Vega, R.; Hoff, C. D. *Inorg. Chem.* **1986**, *25*, 4446−4448.

cleaned, dried in an oven maintained at 145 °C, and then taken into the glovebox. A sample of [PtMe₂(cod)] (**1**; 16.4 mg, 0.05 mmol) was weighed into the lower vessel, which was closed and sealed with 1.5 mL of mercury. A solution of ^{i}PrBABAR-Phos (**2**; 30.2 mg, 0.108 mmol) in CH₂Cl₂ (4 mL) was added, and the remainder of the cell was assembled, removed from the glovebox, and inserted into the calorimeter. The reference vessel was loaded in an identical fashion, with the exception that no platinum complex was added to the lower vessel. After the calorimeter had reached thermal equilibrium at 30.0 °C (ca. 2 h), it was inverted, thereby allowing the reactants to mix. The reaction was considered complete after the calorimeter had once again reached thermal equilibrium (ca. 2 h). Control reactions with Hg and phosphine show no reaction. The enthalpy of ligand substitution (-6.0 ± 0.2 kcal/mol) represents the average of at least three individual calorimetric determinations. The enthalpy of solution of [PtMe₂(cod)] ($+5.8 \pm 0.1$ kcal/mol) in CH₂Cl₂ was determined using identical methodology. This corresponds to a total enthalpy of reaction with all species in solution of -11.8 ± 0.2 kcal/mol. This value can be compared to enthalpy values previously measured for [PtMe₂(PR₃)₂] complexes.[14,15]

(d) X-ray Crystallography. Single crystals of the complex were obtained by slow diffusion of *n*-hexane into a concentrated toluene solution. Crystallographic data for the complex were collected on a Siemens SMART PLATFORM instrument with CCD detector and graphite monochromator and are listed in Table 3. The structure of the complex was solved using direct methods and was refined against full matrix (versus F^2) with SHELXTL (version 5.0).[38] Non-hydrogen atoms were treated anisotropically; hydrogen atoms were refined on calculated positions using the riding model.

(e) Synthesis of [Pt^II Me₂(^{i}PrBABAR-Phos)₂]. A 100 mg (0.3 mmol) portion of [(1,2,5,6-η)-1,5-cyclooctadiene]dimethyl-platinum(II)[39] and 167 mg (0.6 mmol) of ^{i}PrBABAR-Phos[7] were dissolved in 20 mL of methylene chloride. The resulting yellow solution was stirred for 1 h at room temperature. The methylene chloride phase was concentrated to 10% of its volume, and hexane was added to precipitate pure complex (187 mg, 87%). ^{31}P NMR (CD₂Cl₂): δ -69.63 (d, $^{1}J_{PtP} = 1840$ Hz). ^{1}H NMR (CD₂Cl₂): δ 0.90 (d, $^{3}J_{HH} = 6.7$, CH_3 ^{i}Pr, 6H), 0.98 (m, $^{2}J_{PtH} = 78.2$ Hz, $^{3}J_{PH} = 1.6$ Hz, CH_3, 6H), 2.90 (m, $^{2}J_{PH} + ^{4}J_{PH} = 5.1$ Hz, $^{3}J_{PtH} = 9.0$ Hz, PCHCH, 2H), 4.05 (m, $^{3}J_{HH} = 6.7$ Hz, CH ^{i}Pr, 1H), 4.98 (m, $^{3}J_{PH} + ^{6}J_{PH} = 14.3$ Hz, $^{4}J_{PtH} = 11.1$ Hz, CH benzyl, 1H), 6.94–7.20 (m, CH aryl, 8H). ^{13}C NMR (CD₂Cl₂): δ 0.89 (m, CH_3, 1C), 3.01 (m, CH_3, 1C), 21.60 (m, PCHCH, 2C), 22.32 (m, CH_3 ^{i}Pr, 2C), 50.81 (m, CH ^{i}Pr, 1C), 59.55 (m, CH benzyl, 2C), 124.26, 126.06, 127.67, 129.72 (s, CH aryl, 8C), 132.24 (m, quat C, 2C), 136.32 (m, quat C, 2C). Anal. Calcd for C₃₈H₄₂N₂P₂Pt: C, 58.23; H, 5.40. Found: C, 58.34; H, 5.48.

Supporting Information Available: Tables of atomic coordinates and equivalent isotropic displacement parameters, bond distances and angles, anisotropic displacement parameters, and hydrogen coordinates and isotropic displacement parameters for **3** and total energies and complete sets of Cartesian coordinates for the optimized geometries of **4**, **5**, **6a–e**, and **7–10**. This material is available free of charge via the Internet at http://pubs.acs.org.

OM020642Q

(38) Sheldrick, G. M. *Acta Crystallogr., Sect. A* **1990**, *A46*, 467. Sheldrick, G. M. SHELX 97; Universität Göttingen, Göttingen, Germany, 1997.

(39) Costa, E.; Pringle, P. G.; Ravetz, M. *Inorg. Synth. 31*, 284–286; *38*, 1623.